Journal of Biological Engineering

https://doi.org/10.1186/s13036-026-00626-z

Article in Press

Water microdroplet platforms for sustainable, reagent-free viral disinfection

Received: 16 September 2025

Accepted: 13 January 2026

Published online: 03 February 2026

Cite this article as: Sheen J., Lee J., Kim Y. *et al.* Water microdroplet platforms for sustainable, reagent-free viral disinfection. *J Biol Eng* (2026). https://doi.org/10.1186/s13036-026-00626-z

Juyoung Sheen, Jihyun Lee, Yukyung Kim, Kyuhan Lee & Jae Kyoo Lee

Water Microdroplet Platforms for Sustainable, Reagent-Free Viral Disinfection

Juyoung Sheen[1 †], Jihyun Lee[1 †], Yukyung Kim[1], Kyuhan Lee[1], and Jae Kyoo Lee[1,2*]

[1] Department of Applied Bioengineering, Graduate School of Convergence Science and Technology, Seoul National University, Seoul 08826, Republic of Korea

[2] Research Institute for Convergence Science, Seoul National University, Seoul 08826, Republic of Korea.

*Corresponding author E-mail: jaeklee@snu.ac.kr

[†]Equal contributors

Abstract

Background: The repeated emergence of global pandemics has highlighted the urgent need for safe, sustainable, and effective disinfection platforms that eliminate viruses without producing toxic by-products or causing surface damage associated with conventional methods such as ultraviolet irradiation and chemical disinfectants. Here, we present water microdroplet platforms that exploit reactive oxygen species (ROS) spontaneously generated at the air–water interface of micron-sized water droplets, providing a reagent-free and cost-effective approach to viral inactivation. Bacteriophage T7 and lambda (λ), together with MS2 (a non-enveloped RNA bacteriophage) and Phi6 (an enveloped RNA bacteriophage), were selected as model viral systems to evaluate disinfection efficacy across different viral structures.

Results: Water microdroplets with an average diameter of approximately 5 μm, generated by gas nebulization or mesh nebulizers, achieved more than 99.999% viral inactivation within 20 minutes. Transmission electron microscopy, protein profiling, and DNA analyses revealed that microdroplet-derived ROS disrupted viral capsid integrity and degraded nucleic acids, leading to loss of infectivity. The *in situ* generation of multiple ROS species was directly confirmed by mass spectrometry using a TEMPO probe and by fluorescence imaging with ROS-sensitive dyes, while scavenger assays verified the ROS-dependent nature of viral inactivation. Practical feasibility was demonstrated by treating fresh produce surfaces such as lettuce and potato, as well as porous and textile materials, resulting in more than 98% viral inactivation without chemical residues.

Conclusions: Together, these results demonstrate that water microdroplets provide an effective, reagent-free, and environmentally benign viral disinfection strategy with

broad substrate compatibility for applications in food safety, healthcare, and textile-associated environments.

Keywords: water microdroplet platform, Reactive oxygen species, virus inactivation, disinfection, food processing

Background

Viruses are a major threat to human health, causing a wide range of infectious diseases. They are responsible for approximately 15 million deaths annually, accounting for 26 percent of total global mortality(1). The COVID-19 pandemic further underscored the severity and rapid transmission of viral infections, resulting in more than 5.37 million deaths worldwide (2) and a 4.5 percent reduction in the global gross domestic product, equivalent to 3.94 trillion US dollars(3). While vaccines effectively prevent severe disease, the emergence of variants with reduced vaccine responsiveness, together with delayed vaccine distribution in low- and middle-income countries, sustains the global public health risk(4). Therefore, to effectively control viral transmission, there is an urgent engineering challenge to develop sustainable, scalable, and reagent-free disinfection platforms for rapid virus control.

Viruses such as COVID-19 can remain viable on surfaces for extended periods, making effective disinfection essential to reduce indirect transmission, particularly in hospitals where infections threaten patients, healthcare workers, and visitors by prolonging hospitalization, raising costs, and increasing mortality(5-9). In addition, foodborne viruses like rotavirus persist in crops, emphasizing the need for effective disinfection methods to mitigate transmission risks and ensure food safety(10). Notably, rotavirus has been detected in vegetables and crops including sweet potatoes, carrots, radishes, potatoes, and lettuce(11-13).

Current viral disinfection methods usually rely on chemical agents such as sodium hypochlorite, hydrogen peroxide, alcohol-based solutions, and benzalkonium chloride, which

are widely applied in both food processing and healthcare settings(14, 15). However, these disinfectants present major drawbacks, including the formation of toxic by-products, limited efficacy against non-enveloped viruses, adverse health effects, poor biodegradability, and negative environmental impacts(16-20). Thermal and ultraviolet (UV) irradiation are alternative approaches, but their use is limited to unoccupied spaces because of harmful effects on human health and the degradation of environmental surfaces(21). These limitations highlight the engineering need for safe, sustainable, and deployable disinfection technologies.

Recent studies have demonstrated that water-air interface of aqueous microdroplets exhibits unique physicochemical properties distinct from bulk water(22-24), including strong concentration enhancement of solutes (25) and spontaneous formation of intrinsic interfacial electric fields at their surfaces(26). They have been associated with various phenomena, including accelerated reaction rates, spontaneous water oxidation to form reactive oxygen species (ROS), and the reduction of solutes by electrons derived from the oxidation process, all occurring without the need for external catalysts, reductants(27-29). Previous studies have reported that ROS generated from microdroplets along with the droplet surface charge destroyed bacterial cell walls, resulting in effective bacterial inactivation(30-32). The spontaneous generation of ROS from microdroplets using ordinary water offers a promising basis for reagent-free disinfection platforms(20).

Virus disinfection is more difficult than bacterial inactivation because viruses are smaller, allowing easy transmission, and non-enveloped viruses exhibit higher resistance to disinfectants(29). To address this challenge, we sought to translate microdroplet ROS chemistry into a biological engineering platform for virus inactivation. This disruption enables the penetration of ROS into the nucleic acid, resulting in virus inactivation and effective disinfection (Fig.1). We selected bacteriophage T7 and lambda, both non-enveloped and specific to *Escherichia coli*, as well as MS2, a non-enveloped RNA bacteriophage that infects

Escherichia coli, and Phi6, an envelope RNA bacteriophage that infects *Pseudomonas syringae*. Together, these four enable evaluation across RNA and DNA bacteriophages and both non-enveloped and enveloped viral architectures (33-35). Viral disinfection efficacy of bacteriophage T7 and lambda are evaluated using standard plaque assays. The disinfection mechanism is investigated with TEM, SDS-PAGE, and qPCR.

Overall, this study demonstrates that water microdroplet platform provides a practical, scalable, and sustainable disinfection method with direct implications for food processing and healthcare environments.

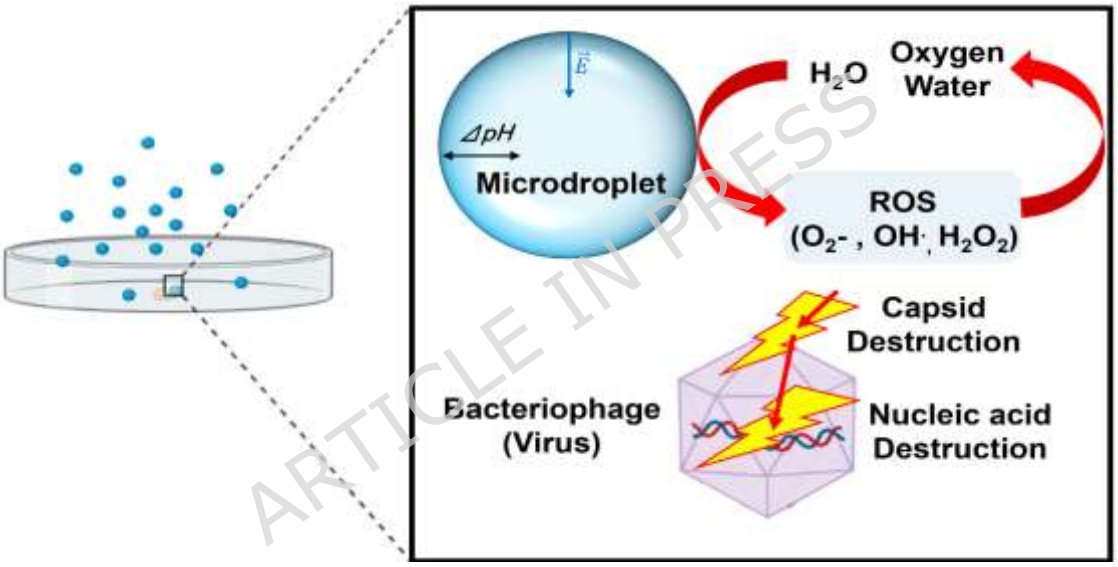

Fig. 1. Schematic illustration of viral disinfection by reactive oxygen species (ROS) generated at the air-water interface of micron-sized droplets.

Methods

Preparation of sample and virus inoculation

Bacteriophage T7 and lambda were purchased from Lysentech (South Korea). Their host strains, Escherichia coli KCTC 1115 and KCTC 1116 (K-12), were used for propagation. LB broth base and LB agar were obtained from Thermo Fisher Scientific (USA). The MS2 and

Phi6 bacteriophages used in this study were kindly provided by Prof. Jae Hee Jung (Sejong University, South Korea). Bacteriophages were loaded on crystal-grade polystyrene Petri dishes (SPL, South Korea). Prior to microdroplet treatment, 5 μL of bacteriophage suspension was deposited and air-dried for 20 minutes. For field tests, fresh lettuce and potatoes were purchased from a local market in Gwanggyo (South Korea). Porous materials, specifically disposable woven cotton cleaning cloths, were purchased from a local market and used to evaluate viral inactivation on porous substrates. Samples were washed with distilled water, surface moisture was removed, and they were cut into $1 \times 1 \times 0.1$ cm^3 squares (Fig. S1). Each sample was exposed to ultraviolet light on both sides to eliminate surface contaminants(10). UV pretreatment was used solely to sterilize background microorganisms on produce surfaces prior to viral inoculation, at an intensity level previously reported to cause no significant surface modification (10). A 5 μL bacteriophage suspension was then inoculated onto each sample and dried for 20 minutes to ensure viral attachment. Although our workflow does not replicate the ISO 15216-1:2017 protocol in full detail, the recovery procedure follows the same functional sequence recommended in the standard—virus detachment, elution into buffer, and collection of eluates for quantitative analysis. Surface-associated viruses were released by immersing lettuce and potato samples in buffer with gentle agitation, and the resulting eluate was directly used for plaque assay–based infectivity measurement.

Microdroplet devices

Microdroplets were generated using two different methods: gas nebulization and a mesh nebulizer. For gas nebulization setup, microdroplets were produced using a 100-μm inner-diameter silica capillary, with a gas pressure of 100 psi. The microdroplet diameter at this setup was estimated to be approximately 5 μm (28). For gas nebulization, deionized water (Sigma-

Aldrich, USA) was introduced into silica capillaries (inner diameter 100 μm). Three capillaries were used simultaneously, each delivering DI water at a flow rate of 10 μL/min via a syringe pump. Nitrogen gas (120 psi) served as the nebulizing agent, generating microdroplets at the capillary tips. For the mesh nebulizer, droplets were generated by vibrating a perforated membrane at high frequency, forcing liquid through micron-sized pores to produce uniform droplets. The device (Tekceleo, France) was equipped with a 5 μm mesh, generating droplets of similar size. The nebulizer flow rate was 0.8 mL/min.

Deposition rate calculation

To enable dose-normalized comparison across exposure times, the deposited microdroplet dose (mL cm^{-2}) was calculated following the framework described by Wood et al. (2021) as:

Deposition rate = $Q \times t / A$

where Q is the spray flow rate (mL min^{-1}), t is the exposure duration (min), and A is the deposition area defined by a 15-mm-diameter region (1.77 cm^2).

Double agar layer assay

A double agar layer assay was performed to assess bacteriophage infectivity based on plaque formation. Host strains were prepared in early stationary-phase culture suspensions. After microdroplet treatment, phages were collected in LB broth and 50 μL of suspension was incubated with the host strain for 15 minutes at room temperature. The mixture was combined with top agar (LB broth containing 0.6 percent agar, preheated to 50°C) and poured onto a bottom agar layer (LB broth with 1.6 percent agar). Plates were incubated at 37°C overnight, and plaques were counted visually. Viral inactivation efficiency was calculated as:

$$\% \text{ virus inactivated} = \frac{P_0 - P_N}{P_0} \times 100 \ ,$$

where P_0 is the plaque number in untreated controls and P_n is the plaque number after n minutes of microdroplet exposure.

Bacteriophage DNA analysis

Digital droplet Polymerase Chain Reaction (ddPCR) (QX200 Droplet Digital PCR, Bio-rad) was conducted to quantitatively analyze the changes in the DNA concentration of bacteriophages before and after microdroplet treatment. DNA of the bacteriophages were extracted by Viral Gene-spin Viral DNA/RNA Extraction kit from iNtRON Biotechnology (South Korea). EvaGreen Supermix (Bio-rad) was used in the ddPCR reactions to enable fluorescence-based quantification of DNA. PCR analysis was performed using specific primers targeting the lambda phage genome: Lambda For (5′-GCG TTA CCG TTT CGC GGT GC-3′) and Lambda Rev (5′-TCG CAG CAT TGC CCG TCA GG-3′)(37, 38).

Transmission Electron Microscopy (TEM)

Microdroplet treated bacteriophage samples and control samples were dropped onto glow charged carbon grids and kept for 10 minutes at room temperature. After the liquid was blotted by filter paper, the grids were covered with 1% uranyl acetate. The transmission electron microscope (TEM) instrument (JEOL, JEM 1010) was utilized with 200 kV at ×25,000 magnification.

SDS-PAGE

T7 and lambda bacteriophages that were untreated or microdroplet treated were mixed with Laemmli buffer (Sigma-Aldrich) and heated for 2 minutes at 85°C. Electrophoresis was performed for 90 minutes at 100 V. After electrophoresis, gels were stained with Coomassie

blue R-250 (Thermo Fisher Scientfic) and scanned using Chemiluminescence Imaging System (iBright CL1500, Thermo Fisher Scientific).

Mass spectrometric analysis

Reactive oxygen species (ROS) generated in water microdroplets were detected using the stable radical probe 2,2,6,6-tetramethylpiperidin-1-oxyl (TEMPO). A 500 μM aqueous TEMPO solution was nebulized into a mass spectrometer inlet using a nitrogen-assisted sprayer (120 psi) at a flow rate of 10 μL/min and a spray distance of 9 cm, matching the conditions used in the viral inactivation assays. ROS-oxidized TEMPO products were analyzed using a Q Exactive Quadrupole–Orbitrap mass spectrometer (Thermo Fisher Scientific). The spray voltage was set to 3 kV, and the inlet temperature was maintained at 250 °C.

Results

Inactivation of Viruses by ROS Generated from Microdroplets

According to the U.S. Centers for Disease Control and Prevention (CDC), a 10-minute contact time is recommended for effective disinfection, and most EPA-registered hospital disinfectants specify this duration on their labels(39). To allow comparison, bacteriophage suspensions were also treated with 100 ppm sodium hypochlorite under the same conditions used for microdroplet exposure.

Viral inactivation by microdroplets was tested using two microdroplet-generation methods: gas nebulization and a mesh nebulizer (Fig. 2). Both approaches produced microdroplets with an average diameter of approximately 5 μm(28). Reactive oxygen species (ROS), including hydrogen peroxide, hydroxyl radicals, and superoxide radicals, were spontaneously generated at the air–water interface of these droplets(20, 28, 40). Deposition rate onto a target surface

was calculated using equation $\text{Deposition rate} = Q \times t/A$. Table S1 summarizes the deposition rate for each device used for microdroplet based viral inactivation. For the gas nebulizer spray (30 μL/min), 10-, 15-, and 20-minute exposures resulted in areal doses of 170, 255, and 340 μL/cm2, respectively. In contrast, the mesh nebulizer (800 μL/min for 10 min) generated a substantially higher deposited dose of 4520 μL/cm2 due to its greater liquid output.

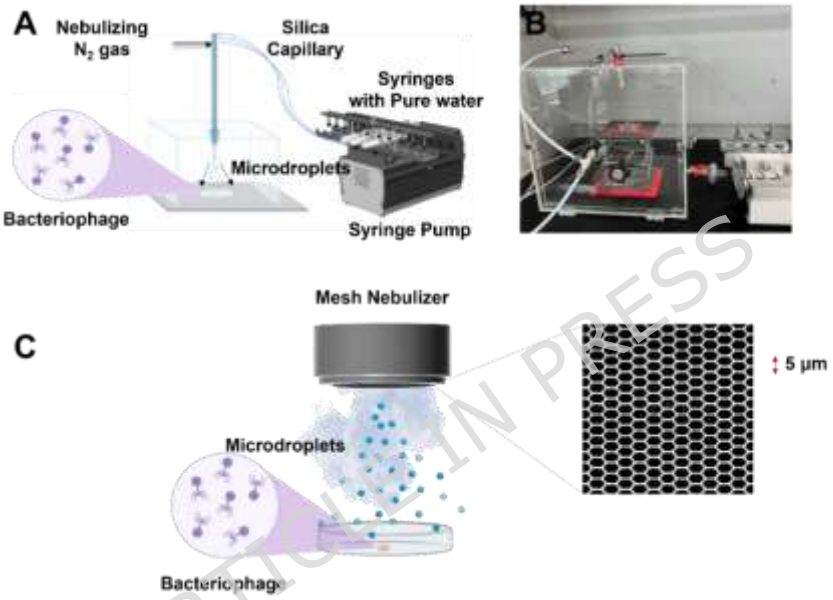

Fig. 2. Experimental setup for microdroplet-based viral disinfection. (A) Schematic of viral disinfection system using a gas nebulizer. (B) Photograph of the microdroplet spraying chamber. (C) Experimental setup of the mesh nebulizer for viral disinfection. Both devices generated microdroplets with an average diameter of approximately 5 μm.

To distinguish the effects of bulk water from those of water microdroplets, an equivalent volume of bulk water was applied to bacteriophage suspensions under the same experimental conditions. To evaluate inactivation efficacy, suspensions were exposed to microdroplet spray for different durations. A pronounced reduction in plaque-forming units (PFUs) was observed in the microdroplet-treated samples compared with both bulk water and untreated controls, as evidenced by visual inspection of plaque assays (Fig. 3A-B). To evaluate whether the antiviral efficacy of microdroplet treatment extends beyond DNA bacteriophages, we tested two RNA

phages with distinct structural properties: MS2, a non-enveloped RNA virus, and Phi6, an enveloped RNA virus. As shown in Fig. 3C–D, MS2 produced dense plaques in untreated controls and exhibited only limited reduction with bulk water, whereas microdroplet treatment resulted in near-complete plaque disappearance. Phi6 showed similarly high susceptibility to microdroplet treatment, with substantial loss of plaques relative to both untreated and bulk-water conditions.

A time-dependent study was performed by exposing bacteriophage suspensions to microdroplet treatment for different durations, which revealed progressively higher inactivation with longer exposure (Fig. 3E, Fig. S2). Viral infectivity was quantified by counting plaque-forming units (PFUs) after incubation. Raw plaque counts, PFU/mL calculations, and assay limits of detection corresponding to Figs. 3 and 6 are provided in Tables S2-S5. In Fig. 3E, lambda phage displayed a gradual decline in infectivity, reaching more than six log reductions after 15 minutes of microdroplet exposure. In contrast, T7 remained relatively resistant during the first 10 minutes, but then underwent a sharp decline between 15 and 20 minutes, consistent with cumulative ROS-induced capsid damage. These differences may be attributed to structural and physicochemical distinctions between the two phages, with lambda being more vulnerable to early ROS-mediated capsid oxidation, whereas T7 resists initial oxidative stress but undergoes accelerated inactivation after prolonged exposure due to accumulated structural damage. This observation is consistent with previous reports that bacteriophage T7 exhibits higher oxidative stress resistance compared with bacteriophage MS2 and *E. coli(34)*.

We compared the antiviral efficacy of microdroplets with sodium hypochlorite (NaClO) under identical conditions (Fig. 3F-G). After 10 minutes of treatment, microdroplets achieved 99.16 percent inactivation for T7 and 99.56 percent for lambda. Sodium hypochlorite was less effective against T7 but showed strong activity against lambda, whereas microdroplets

provided the highest level of inactivation for both bacteriophages. Quantitative analysis (Fig. 3H–I) further confirmed that microdroplets achieved greater than 99 percent inactivation for both RNA phages (MS2 and Phi6), outperforming bulk water and showing efficacy comparable to NaClO treatment.

These findings demonstrate that microdroplet treatment is more effective than chlorine-based disinfectants within the same exposure time and volume. Moreover, the marked difference between bulk water and microdroplets highlights that the antiviral activity originates from the unique physicochemical properties of microdroplets, particularly their ability to generate reactive oxygen species at the air–water interface.

To benchmark the microdroplet platform against commonly used chemical disinfectants, we compared its antiviral efficacy with ethanol, hydrogen peroxide, and sodium hypochlorite. As shown in Supplementary Fig. S3A–B, microdroplet spraying achieved the highest level of inactivation for MS2 (99.71 percent), whereas ethanol, hydrogen peroxide, and sodium hypochlorite achieved inactivation efficiencies of 97.45, 95.75, and 97.91 percent, respectively. For Phi6, microdroplet treatment reached 99.25 percent inactivation, compared with 97.56–98.20 percent for the chemical disinfectants. These results demonstrate that the microdroplet platform performs comparably to, or better than, widely used chemical disinfectants while requiring only water and leaving no chemical residues. Environmental factors known to influence ROS generation, including nebulization gas composition (ambient air, O_2, and N_2) and relative humidity (40 percent and 60 percent), did not significantly affect antiviral outcomes. As shown in Fig. S4A–D, both MS2 (97.65–98.93 percent) and Phi6 (98.74–99.51 percent) remained highly susceptible under all tested conditions, indicating robust

microdroplet-mediated disinfection performance across diverse environmental settings.

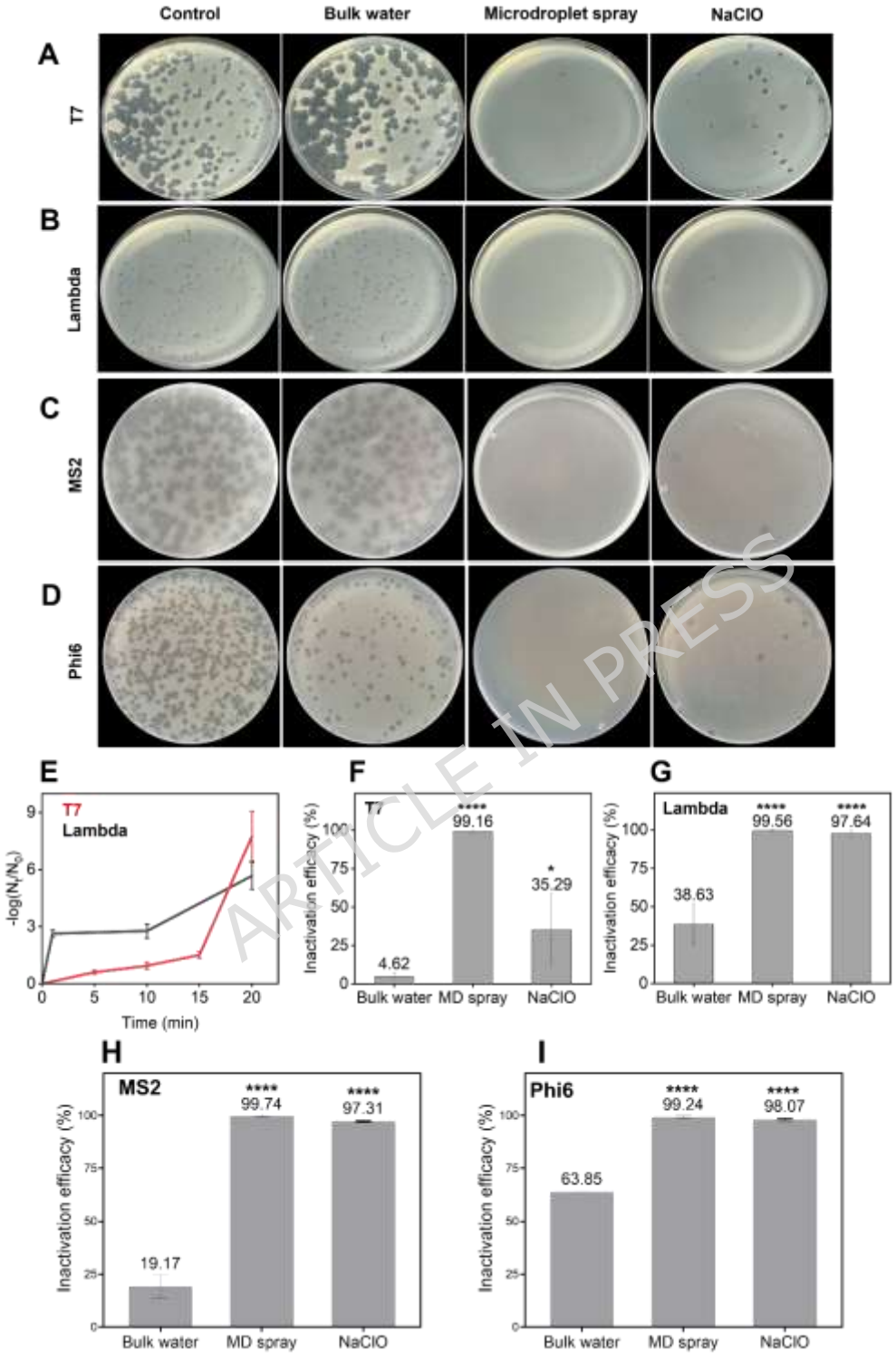

Fig. 3. Inactivation of non-enveloped DNA bacteriophages (T7 and lambda), non-enveloped RNA bacteriophage (MS2), and enveloped RNA bacteriophage (Phi6) by water microdroplet treatment. (A,B) Representative plaque assay images of T7 (A) and lambda (B) after 10 minutes of treatment with bulk water, microdroplet spray, or sodium hypochlorite (NaClO, 100 ppm), compared with untreated controls. (C,D) Representative plaque assay

images of MS2 (C) and Phi6 (D) under the same treatment conditions. (E) Time-dependent viral inactivation under microdroplet exposure. Lambda (gray) shows a gradual decline, whereas T7 (red) remains stable until 10 minutes and then decreases sharply between 15 and 20 minutes. (F) Percent inactivation of T7 after 10 minutes for bulk water, microdroplets, and NaClO. (G) Percent inactivation of lambda after 10 minutes for bulk water, microdroplets, and NaClO. (H,I) Quantification of MS2 (H) and Phi6 (I) inactivation efficiencies after 10 minutes of treatment. Error bars indicate standard deviations from triplicate experiments. Statistical significance was assessed using one-way ANOVA with post-hoc multiple comparison tests (* $p < 0.05$, ** $p < 0.01$, *** $p < 0.001$, **** $p < 0.0001$).

Morphological Changes in Microdroplet-treated Bacteriophages

To determine whether ROS generated from microdroplets disrupt viral capsid structures, transmission electron microscopy (TEM) was used to compare the morphology of untreated and microdroplet-treated bacteriophages (Fig. 4, Fig. S5). Total six virus particles analyzed in the TEM images for morphological assessments. Viral particles were analyzed per condition in the TEM micrographs. Damage categories were defined based on (i) capsid integrity—loss of icosahedral geometry, surface disruption, or structural collapse—and (ii) tail morphology, including detachment or deformation. Untreated controls showed intact viral particles with well-defined capsids. For T7, the average head diameter of five representative particles was approximately 62 nm, consistent with reported dimensions (Fig. 4A). Lambda phage exhibited a defined head structure with an average diameter of 66 nm and a tail length of 137 nm. (Fig. 4B)

In contrast, microdroplet-treated samples (Fig. 4B,C,E,F) displayed disrupted and aggregated particles, with evident loss of capsid integrity, indicating significant structural damage caused by ROS. These alterations are consistent with previous observations of ROS-mediated disruption in bacteriophages (41, 42).

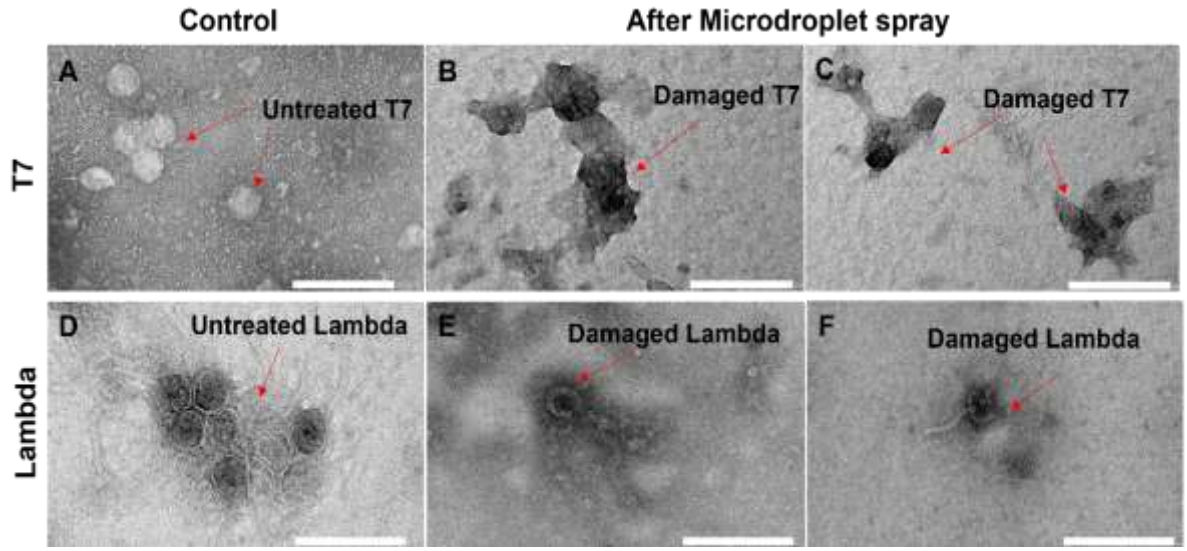

Fig. 4. Morphological changes in bacteriophages after microdroplet treatment. (A) Untreated T7 showing intact head and tail structures. (B, C) T7 after microdroplet exposure, displaying disrupted and aggregated morphology. (D) Untreated lambda showing intact head and tail. (E, F) Lambda after microdroplet treatment, exhibiting damaged head and tail proteins. Scale bars, 200 nm.

Mechanisms of Microdroplet-induced Viral disinfection

Next, we investigated the mechanism of bacteriophage inactivation by microdroplet treatment. SDS-PAGE analysis was performed to examine whether the structural degradation observed after microdroplet exposure was associated with degradation of viral proteins (Fig. 5A). Protein bands of bacteriophages treated with microdroplets for 10 minutes appeared markedly fainter than those of untreated controls, indicating substantial protein loss or degradation. The reduced band intensity is likely due to ROS-induced denaturation and aggregation of capsid proteins, which hindered migration through the gel or caused protein loss during sample preparation. Densitometric quantification of the major capsid protein bands revealed a greater than 90 percent reduction in relative protein intensity following microdroplet treatment (Fig. 5B), indicating extensive ROS-induced oxidative damage and structural disruption at the protein

level. This interpretation is supported by TEM observations (Fig. 4), which revealed extensive capsid disruption in microdroplet-treated samples.

The loss of capsid integrity suggests that viral nucleic acids became exposed and were subsequently damaged. To test this, ddPCR was conducted to quantify DNA concentration before and after microdroplet treatment (Fig. 5C). Lambda DNA concentration decreased from 7.73 to 5.53 copies/μL, consistent with partial genome degradation. This reduction is attributed to oxidative damage by ROS, which can cause DNA fragmentation and loss of genetic material.

To verify that these structural and genomic damages originate from microdroplet-generated ROS, we directly characterized the ROS generated from microdroplets Mass spectrometric analysis using the ROS-sensitive probe TEMPO, performed under the same spray conditions as the viral inactivation assays (9 cm, 120 psi), revealed clear formation of TEMPO–OH and TEMPO–OOH (Fig. S6A), confirming in situ generation of hydroxyl and hydroperoxyl/superoxide species. To further visualize ROS formation within individual microdroplets, we employed fluorescence microscopy using three ROS-responsive dyes: PF1 for H_2O_2, HPF for •OH, and DHE for superoxide. As shown in Fig. S6B, microdroplets produced strong punctate fluorescence across all dye conditions, indicating that each ROS species is generated directly within the droplets. These mass spectrometric and fluorescence measurements together establish that microdroplets generate a spectrum of ROS species capable of inducing the observed capsid and genome damages in bacteriophages.

Then, we employed scavenger assays targeting $O_2^{\bullet -}$ (SOD), •OH (salicylic acid), and solvated electrons (sodium nitrate). Figure 5D shows inactivation efficacy of microdroplets containing each ROS scavenger, which shows significantly reduced inactivation efficiency in the presence of ROS scavengers. For comparison, bulk water treatments showed minimal changes in viral infectivity (Fig. S7), indicating that ROS-driven inactivation is specific to microdroplet rather than bulk water. In the case of SOD, the higher inactivation efficacy may

be explained by the conversion of superoxide radicals into hydrogen peroxide, rather than by complete suppression of ROS. Previous studies have reported that elevated SOD activity can paradoxically increase oxidant toxicity by accelerating H_2O_2 formation and enhancing susceptibility to oxidative damage, supporting the possibility that SOD alters rather than eliminates ROS burden (43, 44). These results together confirm that ROS spontaneously generated from microdroplets acts as a virucide.

Collectively, these results demonstrate that reactive oxygen species generated from water microdroplets are both necessary and sufficient to induce capsid disruption and genome damage, leading to irreversible viral inactivation. Based on these findings, we propose an integrated mechanism for microdroplet-mediated viral disinfection, as summarized in Fig. 6.

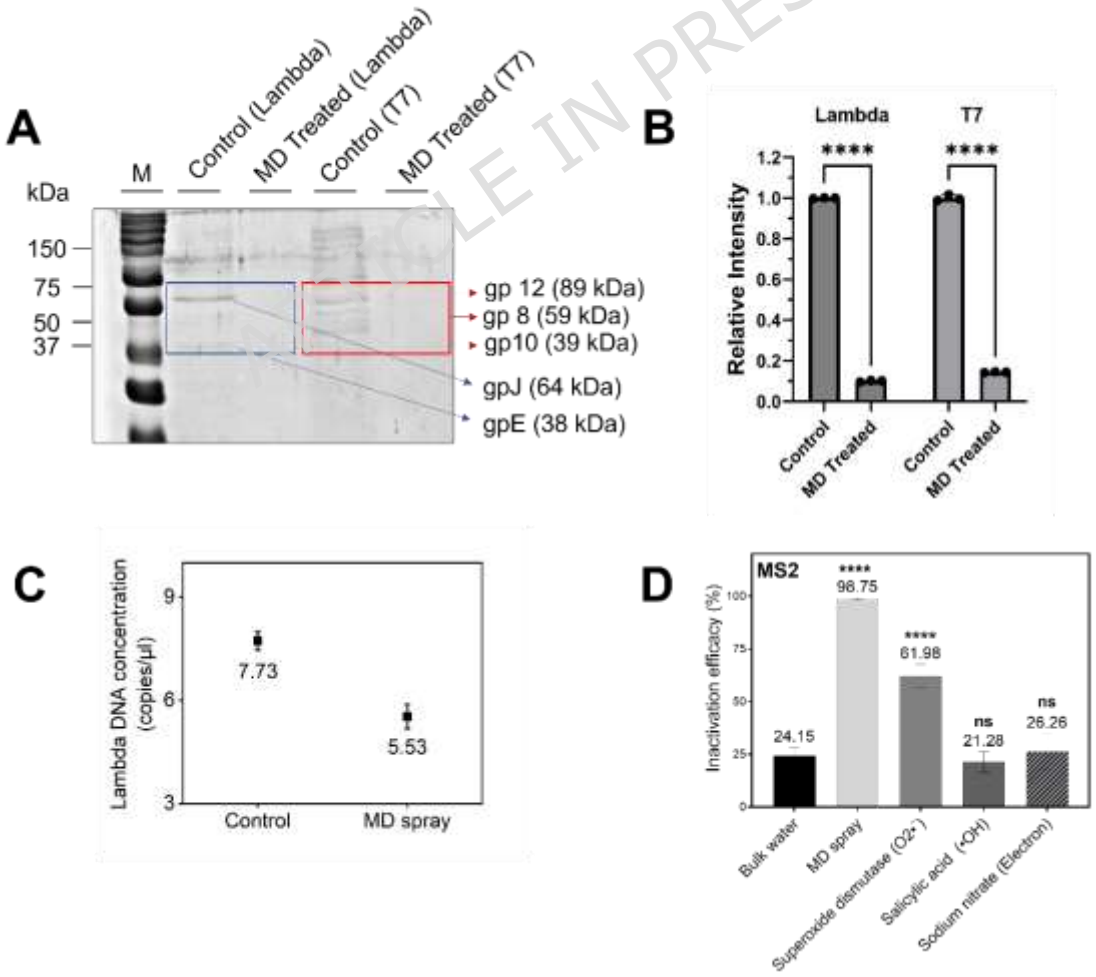

Fig. 5. Microdroplet-generated reactive oxygen species (ROS) induce capsid degradation, genome damage, and ROS-dependent loss of infectivity in bacteriophages. (A) SDS-PAGE analysis of viral proteins. Blue Box: major lambda capsid protein (gpE) and tail fiber protein (gpJ). Red box: T7 capsid head protein (gp10) and tail proteins (gp8, gp12). Bands are markedly fainter in microdroplet-treated samples, indicating protein degradation and aggregation. (B) Quantification of capsid protein degradation after microdroplet treatment based on densitometric analysis of SDS-PAGE bands. (C) ddPCR analysis of lambda genomic DNA concentration, showing a decrease from 7.73 to 5.53 copies per μL after microdroplet treatment, consistent with oxidative genome damage. Error bars represent standard deviations from three independent replicates. (D) Effects of ROS scavengers on microdroplet-mediated viral inactivation. Superoxide dismutase (SOD; superoxide scavenger), salicylic acid (·OH scavenger), and sodium nitrate (electron scavenger) reduced antiviral efficacy to varying extents, demonstrating the involvement of multiple ROS pathways during microdroplet treatment. Error bars denote standard deviations (n = 3). Statistical significance was evaluated using one-way ANOVA with post-hoc multiple comparison tests (* $p < 0.05$, ** $p < 0.01$, *** $p < 0.001$, **** $p < 0.0001$); "ns" indicates non-significant differences relative to the bulk water treatment control.

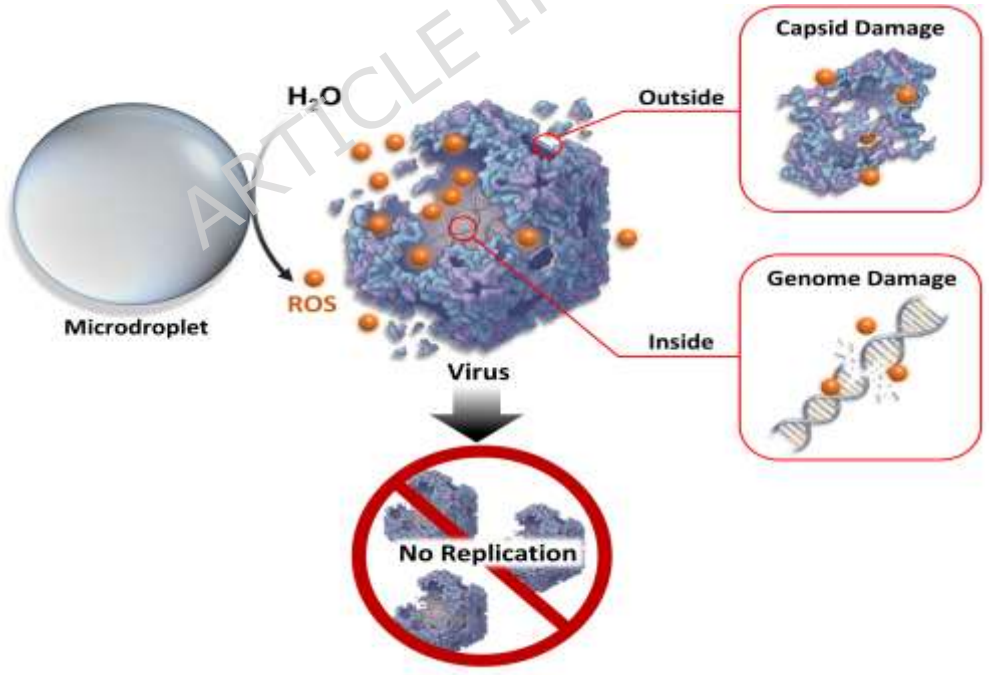

Fig. 6. Proposed mechanism of virus inactivation by water microdroplets. ROS generated at the air-water interface oxidizes viral capsid proteins, compromise structural integrity, and damage nucleic acids, leading to complete loss of infectivity.

Viral Disinfection on Food Surfaces and Porous Materials using Water Microdroplets

To assess the practical applicability of microdroplet-mediated viral disinfection across materials relevant to real-world transmission, we evaluated antiviral efficacy on both food surfaces and porous substrates, including fresh produce and woven textile materials. Lettuce is a major vehicle for the transmission of enteric viruses such as rotavirus in the United States, because it is often consumed raw and its broad, uneven surface facilitates viral adherence and limits the effectiveness of washing (10). In addition, previous studies have shown that rotavirus can be transmitted to humans through irrigated crops including carrots, potatoes, and sweet potatoes (12). These findings highlight the need for effective disinfection strategies that can be applied to a variety of fresh foods.

To evaluate the applicability of microdroplet treatment in food systems, viruses were directly inoculated onto the surfaces of lettuce and potato samples. Figure 7A shows a schematic of the experimental procedure. Lettuce leaves and potato slices were cut into 1 × 1 × 0.1 cm^3 squares, exposed to ultraviolet light on both sides to remove pre-existing contaminants (10), and then inoculated with 5 μL of bacteriophage suspension. After drying for 20 minutes, the inoculated samples were treated with microdroplet spray for 10 minutes.

Following treatment, viruses were recovered from the food surfaces and assessed by plaque assay (Fig. 7B). Inactivation efficacy on lettuce was similar to that observed for Petri dish surfaces (Fig. 7C, D), indicating that the antiviral effect of microdroplets is maintained across different substrates. On potato skin, despite its irregular and curved surface, microdroplet treatment also resulted in effective inactivation (Fig. 7E). Overall, microdroplet treatment achieved more than 98.9 percent inactivation of T7 on both lettuce and potato surfaces (Fig. 7F), demonstrating robust antiviral efficacy regardless of surface characteristics. Finally, we compared spray-based and mesh-nebulizer systems (Fig. 7G). Both methods achieved

379 comparable inactivation efficiencies, 98.99 percent and 97.17 percent, respectively, indicating
380 that antiviral efficacy depends primarily on droplet size rather than generation method.

381 Because porous materials such as textiles can act as reservoirs for viral particles and are
382 challenging to disinfect using conventional surface treatments, we further evaluated the
383 microdroplet platform on porous substrates using woven cotton fabric. Both MS2 and Phi6
384 exhibited greater than 99 percent inactivation on fabric surfaces despite their high absorbency
385 and structural heterogeneity (Fig. 7H–J). These results indicate that microdroplet-generated
386 ROS can effectively penetrate and disinfect porous materials, extending the practical

applicability of the platform beyond non-porous and food-contact surfaces to textiles and other high-porosity environments.

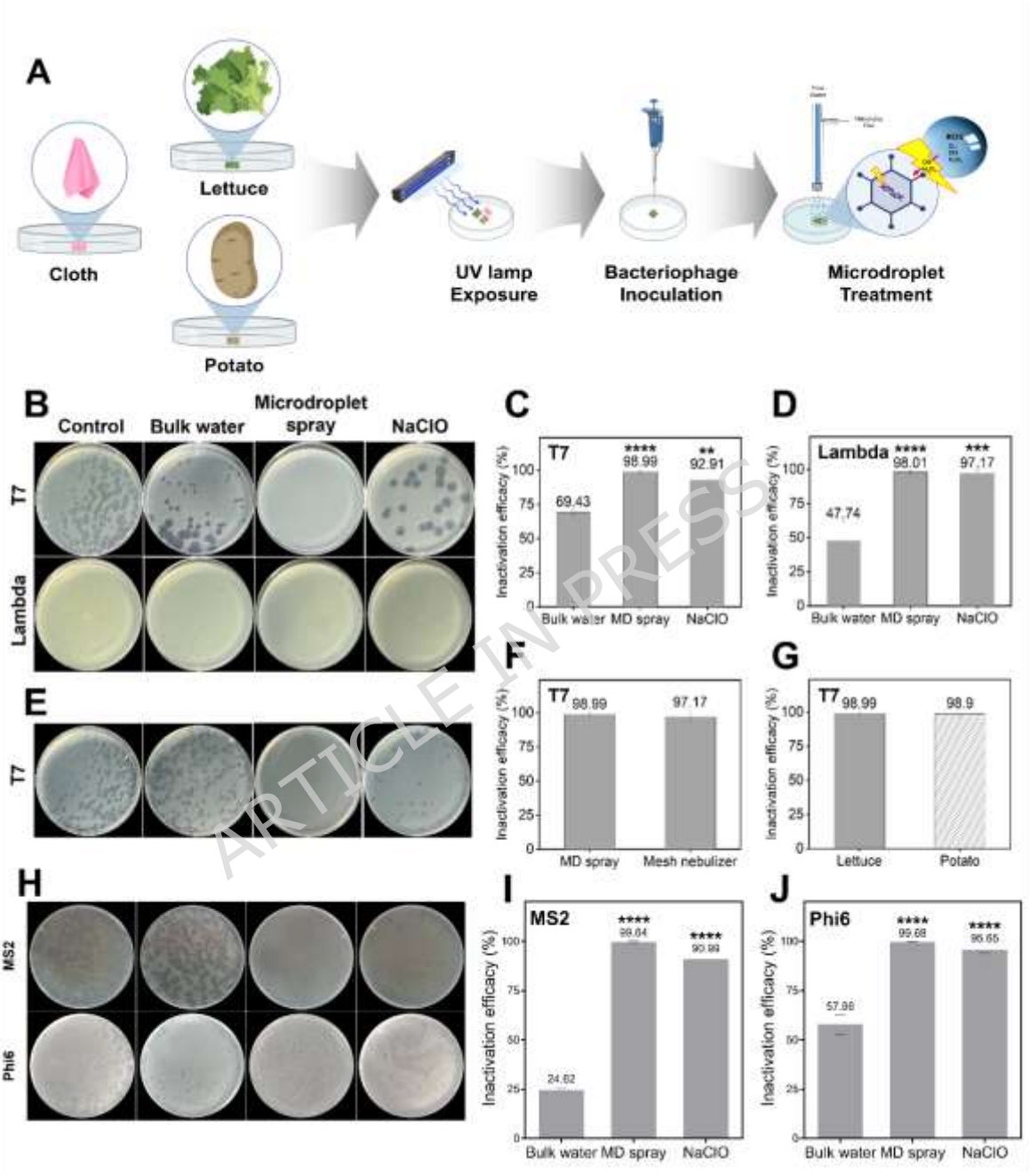

Fig. 7. Disinfection of food surfaces and porous materials using water microdroplets. (A) Schematic of the experimental procedure. (B) Plaque assay of bacteriophages on lettuce after microdroplet treatment. (C, D) Inactivation efficacy on lettuce: T7, 98.99 percent; lambda, 98.01 percent. (E) Plaque assay of T7 on potato after microdroplet treatment. (F) Inactivation efficacies of T7 on lettuce and potato were 98.99 and 98.9 percent, respectively. (G) Comparison of droplet generation methods showing similar inactivation

efficacy: microdroplet spray, 98.99 percent; mesh nebulizer, 97.17 percent. (H) Representative plaque assay images of MS2 and Phi6 deposited on woven textile surfaces following treatment with bulk water, microdroplet spray, or NaClO, compared with untreated controls. (I,J) Quantification of inactivation efficacy for MS2 (I) and Phi6 (J) on textile surfaces under the same treatment conditions. Error bars represent standard deviations from three independent replicates. Statistical significance was assessed using one-way ANOVA with post-hoc multiple comparison tests (* $p < 0.05$, ** $p < 0.01$, *** $p < 0.001$, **** $p < 0.0001$).

Discussion

Virus inactivation using ROS generated from water microdroplets represents a novel, cost-effective, and non-hazardous disinfection strategy. In contrast, conventional chemical disinfectants are limited by their selective reactivity and the formation of harmful by-products. For example, chlorine-based disinfectants react with organic compounds in a highly selective manner, targeting specific sites on aromatic rings depending on molecular structure (45) and produce toxic disinfection by-products such as trihalomethanes (THMs)(46). These issues raise concerns over chemical safety and sustainability.

Unlike chemical agents, microdroplet-generated ROS interact broadly with biomolecules, including lipids and nucleic acids (47). Moreover, this method requires only ordinary water, eliminating the risk of hazardous residues. Because ROS decompose into water and oxygen after reaction, microdroplet disinfection is inherently safe for both humans and the environment (20). Together, these properties overcome the drawbacks of current disinfectants, including chemical toxicity, low biodegradability, and environmental burden.

The present study demonstrated that microdroplet treatment achieved more than 99 percent inactivation of bacteriophages across different surfaces, including plastics and fresh produce, underscoring its applicability in real-world settings such as food processing and healthcare environments. This high efficacy, combined with the absence of chemical additives, positions

420 microdroplet technology as a safe and eco-friendly alternative to chlorine-based disinfectants
421 and UV irradiation.

422 The operational simplicity and low cost of microdroplet generation make this platform
423 highly scalable and accessible. Unlike UV systems that require high capital investment or
424 chlorine-based methods with ongoing maintenance, microdroplet systems rely only on water
425 and minimal energy input. A preliminary cost analysis indicates that the microdroplet-ROS
426 process operates at approximately 0.0007–0.0009 US$/min, consuming only distilled water
427 and compressed gas (48, 49). A detailed comparison with UV and chlorine disinfection costs
428 is provided in Table S6. Future development could focus on continuous-flow chambers,
429 integration into HVAC or conveyor systems, and coupling with biosensor for real-time
430 monitoring. Taken together, our findings establish microdroplet ROS disinfection as not only
431 an eco-friendly alternative but also a scalable platform for virus control in food safety and
432 healthcare environments.

433

434 ## Conclusions

435 This study demonstrates that ROS generated from water microdroplets effectively inactivate
436 bacteriophages, including T7 and lambda, through capsid protein and nucleic acid damage. The
437 antiviral efficiency was confirmed across various surfaces, with virus inactivation efficacies
438 exceeding 99%, even on irregular or curved food surfaces. In time-dependent experiments,
439 more than 5-log reductions in viral infectivity were achieved with prolonged microdroplet
440 treatment, indicating more than 99.999% bacteriophage inactivation. Because microdroplets
441 are produced from ordinary water and yield only non-toxic by-products, this approach offers a
442 safe, sustainable, and cost-effective alternative to chemical disinfectants. These findings

443 establish water microdroplet platforms as a practical, scalable, and sustainable disinfection
444 technology with direct applications in food safety and healthcare environments.
445
446 ## Supplementary Information
447 Supplementary data supporting this article are provided as additional files.
448
449 ## Declarations
450 **Ethics approval and consent to participate**
451 Not applicable.
452
453 **Consent for publication**
454 All authors approved the final manuscript and the submission to this journal.
455
456
457
458 **Availability of data and materials**
459 The datasets supporting the conclusions of this article are included within the article and its
460 additional files.
461
462 **Competing interests**
463 The authors declare that they have no competing interests.
464
465 **Funding**

This work was supported by the National Research Foundation of Korea (NRF) grant funded by the Korea government (MSIT)(2023R1A2C200723812). This research was supported by Basic Science Research Program through the National Research Foundation of Korea (NRF) funded by the Ministry of Education(2022R1A6A1A03063039). This work was supported by the LAMP Program of the National Research Foundation of Korea (NRF) grant funded by the Ministry of Education (No. RS-2023-00301976). This work was supported by Creative-Pioneering Researchers Program through Seoul National University, Basic Science Research Program through the National Research Foundation of Korea (NRF) funded by the Ministry of Education (2022R1A6A1A0306303911).

Authors' contributions

J.S. and J.L contributed equally to this work. J.K.L and J.S. designed the project. J.S. and J.L. performed all bacteriophage experiments. Y.K. performed and analyzed the protein experiments. J.S. and J.L. analyzed and interpreted the data. J.S., J.L., and J.K.L wrote the manuscript.

Acknowledgements

We gratefully acknowledge Prof. Jae Hee Jung (Sejong University, South Korea) for kindly providing the MS2 and Phi6 bacteriophages used in this study.

References

1. Fauci AS, Morens DM. The Perpetual Challenge of Infectious Diseases. New England Journal of Medicine. 2012;366(5):454–61.
2. Koopmans M. Noroviruses in healthcare settings: a challenging problem. J Hosp Infect. 2009;73(4):331–7.
3. Scott RD. The Direct medical costs of healthcare-associated infections in U.S. hospitals and the benefits of prevention. 2009.
4. Lopman BA, Hall AJ, Curns AT, Parashar UD. Increasing rates of gastroenteritis hospital discharges in US adults and the contribution of norovirus, 1996-2007. Clin Infect Dis. 2011;52(4):466–74.

5. Bartsch SM, Lopman BA, Ozawa S, Hall AJ, Lee BY. Global Economic Burden of Norovirus Gastroenteritis. PLoS One. 2016;11(4):e0151219.
6. Zingg W, Colombo C, Jucker T, Bossart W, Ruef C. Impact of an outbreak of norovirus infection on hospital resources. Infect Control Hosp Epidemiol. 2005;26(3):263–7.
7. Klevens RM, Edwards JR, Richards CL, Jr., Horan TC, Gaynes RP, Pollock DA, et al. Estimating health care-associated infections and deaths in U.S. hospitals, 2002. Public Health Rep. 2007;122(2):160–6.
8. Harris JP, Adak GK, O'Brien SJ. To close or not to close? Analysis of 4 year's data from national surveillance of norovirus outbreaks in hospitals in England. BMJ Open. 2014;4(1):e003919.
9. Aitken C, Jeffries DJ. Nosocomial spread of viral disease. Clin Microbiol Rev. 2001;14(3):528–46.
10. Han S, Song MS, Song H, Yu J, Choi C, Park SH, et al. Control of rotavirus by sequential stress of disinfectants and gamma irradiation in leafy vegetable industry. Food Res Int. 2025;200:115456.
11. Jones RM, Brosseau LM. Aerosol transmission of infectious disease. J Occup Environ Med. 2015;57(5):501–8.
12. Gadelha J, Allende A, Lopez Galvez F, Fernández, Gil M, Fenández P. Chemical risks associated to ready-to-eat vegetables: quantitative analysis to estimate disinfection-by-products during washing2019.
13. Fears AC, Klimstra WB, Duprex P, Hartman A, Weaver SC, Plante KS, et al. Persistence of Severe Acute Respiratory Syndrome Coronavirus 2 in Aerosol Suspensions. Emerg Infect Dis. 2020;26(9):2168–71.
14. Yasugi M, Komura Y, Ishigami Y. Mechanisms underlying inactivation of SARS-CoV-2 by nano-sized electrostatic atomized water particles. J Nanopart Res. 2022;24(5):99.
15. Kampf G, Todt D, Pfaender S, Steinmann E. Persistence of coronaviruses on inanimate surfaces and their inactivation with biocidal agents. J Hosp Infect. 2020;104(3):246–51.
16. Eggers M, Suchomel M. In-vivo efficacy of alcohol-based hand rubs against noroviruses: a novel standardized European test method simulating practical conditions. J Hosp Infect. 2023;135:186–92.
17. Gil MI, López-Gálvez F, Andújar S, Moreno M, Allende A. Disinfection by-products generated by sodium hypochlorite and electrochemical disinfection in different process wash water and fresh-cut products and their reduction by activated carbon. Food Control. 2019;100:46–52.
18. Xiao S, Yuan Z, Huang Y. Disinfectants against SARS-CoV-2: A Review. Viruses. 2022;14(8).
19. Bogdan J, Zarzynska J, Plawinska-Czarnak J. Comparison of Infectious Agents Susceptibility to Photocatalytic Effects of Nanosized Titanium and Zinc Oxides: A Practical Approach. Nanoscale Res Lett. 2015;10(1):1023.
20. Dulay MT, Lee JK, Mody AC, Narasimhan R, Monack DM, Zare RN. Spraying Small Water Droplets Acts as a Bacteriocide. QRB Discov. 2020;1:e3.
21. Otter JA, Donskey C, Yezli S, Douthwaite S, Goldenberg SD, Weber DJ. Transmission of SARS and MERS coronaviruses and influenza virus in healthcare settings: the possible role of dry surface contamination. Journal of Hospital Infection. 2016;92(3):235–50.
22. Daly R, Sader JE, Boland JJ. Existence of Micrometer-Scale Water Droplets at Solvent/Air Interfaces. Langmuir. 2012;28(37):13218–23.
23. Kunding AH, Busk LL, Webb H, Klafki HW, Otto M, Kutter JP, et al. Micro-droplet arrays for micro-compartmentalization using an air/water interface. Lab on a Chip. 2018;18(18):2797–805.
24. Rao Z, Fang Y-G, Pan Y, Yu W, Chen B, Francisco JS, et al. Accelerated Photolysis of H2O2 at the Air–Water Interface of a Microdroplet. Journal of the American Chemical Society. 2023;145(45):24717–23.
25. Xiong H, Lee JK, Zare RN, Min W. Strong Concentration Enhancement of Molecules at the Interface of Aqueous Microdroplets. J Phys Chem B. 2020;124(44):9938–44.
26. Xiong H, Lee JK, Zare RN, Min W. Strong Electric Field Observed at the Interface of Aqueous Microdroplets. J Phys Chem Lett. 2020;11(17):7423–8.
27. Lee JK, Samanta D, Nam HG, Zare RN. Spontaneous formation of gold nanostructures in aqueous microdroplets. Nat Commun. 2018;9(1):1562.
28. Lee JK, Walker KL, Han HS, Kang J, Prinz FB, Waymouth RM, et al. Spontaneous generation of hydrogen peroxide from aqueous microdroplets. Proc Natl Acad Sci U S A. 2019;116(39):19294–8.
29. Nakano R, Hara M, Ishiguro H, Yao Y, Ochiai T, Nakata K, et al. Broad Spectrum Microbicidal Activity of Photocatalysis by TiO2. Catalysts. 2013;3(1):310–23.
30. Vatansever F, de Melo WC, Avci P, Vecchio D, Sadasivam M, Gupta A, et al. Antimicrobial strategies centered around reactive oxygen species--bactericidal antibiotics, photodynamic therapy, and beyond. FEMS Microbiol Rev. 2013;37(6):955–89.

31. Pillet F, Formosa-Dague C, Baaziz H, Dague E, Rols M-P. Cell wall as a target for bacteria inactivation by pulsed electric fields. Scientific Reports. 2016;6(1):19778.
32. Pyrgiotakis G, Vasanthakumar A, Gao Y, Eleftheriadou M, Toledo E, DeAraujo A, et al. Inactivation of foodborne microorganisms using engineered water nanostructures (EWNS). Environ Sci Technol. 2015;49(6):3737–45.
33. Clark EM, Wright H, Lennon K-A, Craik VA, Clark JR, March JB. Inactivation of recombinant bacteriophage lambda by use of chemical agents and UV radiation. Applied and Environmental Microbiology. 2012;78(8):3033–6.
34. Mamane H, Shemer H, Linden KG. Inactivation of E. coli, B. subtilis spores, and MS2, T4, and T7 phage using UV/H2O2 advanced oxidation. Journal of hazardous materials. 2007;146(3):479–86.
35. Singh D, Dimri AG, Pandey A, Nayak SK, Bhat B, Das M. Analysis of biocidal efficacies of various disinfectant systems against bacteria, fungi and bacteriophage lambda: A comparative assessment. Biomedical and Therapeutics Letters. 2024;11(2):915–.
36. Wood JP, Magnuson M, Touati A, Gilberry J, Sawyer J, Chamberlain T, et al. Evaluation of electrostatic sprayers and foggers for the application of disinfectants in the era of SARS-CoV-2. PloS one. 2021;16(9):e0257434.
37. Edelman DC, Barletta J. Real-time PCR provides improved detection and titer determination of bacteriophage. BioTechniques. 2003;35(2):368–75.
38. Refardt D. Real-time quantitative PCR to discriminate and quantify lambdoid bacteriophages of Escherichia coli K-12. Bacteriophage. 2012;2(2):98–104.
39. Voorn MG, Kelley AM, Chaggar GK, Li X, Teska PJ, Oliver HF. Contact time and disinfectant formulation significantly impact the efficacies of disinfectant towelettes against Candida auris on hard, non-porous surfaces. Sci Rep. 2023;13(1):5849.
40. Lee JK, Samanta D, Nam HG, Zare RN. Micrometer-Sized Water Droplets Induce Spontaneous Reduction. J Am Chem Soc. 2019;141(27):10585–9.
41. Guo L, Xu R, Gou L, Liu Z, Zhao Y, Liu D, et al. Mechanism of Virus Inactivation by Cold Atmospheric-Pressure Plasma and Plasma-Activated Water. Appl Environ Microbiol. 2018;84(17).
42. Gelderblom HR, Biel S. Electron microscopy of viruses. In: Cann AJ, editor. Virus Culture: A Practical Approach: Oxford University Press; 1999. p. 0.
43. Nosaka Y, Nosaka AY. Generation and Detection of Reactive Oxygen Species in Photocatalysis. Chem Rev. 2017;117(17):11302–36.
44. Scott MD, Meshnick SR, Eaton JW. Superoxide dismutase-rich bacteria. Paradoxical increase in oxidant toxicity. Journal of Biological Chemistry. 1987;262(8):3640–5.
45. Wang T, Deng L, Tan C, Hu J, Prasad Singh R. Reaction mechanisms of chlorinated disinfection byproducts formed from nitrophenol compounds with different structures during chlor(am)ination and UV/post-chlor(am)ination. Journal of Hazardous Materials. 2024;472:134544.
46. Tak S, Kumar A. Chlorination disinfection by-products and comparative cost analysis of chlorination and UV disinfection in sewage treatment plants: Indian scenario. Environmental Science and Pollution Research. 2017;24(34):26269–78.
47. Han L, Patil S, Boehm D, Milosavljević V, Cullen PJ, Bourke P. Mechanisms of Inactivation by High-Voltage Atmospheric Cold Plasma Differ for Escherichia coli and Staphylococcus aureus. Appl Environ Microbiol. 2016;82(2):450–8.
48. Collivignarelli MC, Abba A, Miino MC, Caccamo FM, Torretta V, Rada EC, et al. Disinfection of Wastewater by UV-Based Treatment for Reuse in a Circular Economy Perspective. Where Are We at? Int J Environ Res Public Health. 2020;18(1).
49. Pelayo D, Rivero MJ, Santos G, Gomez P, Ortiz I. Techno-economic evaluation of UV light technologies in water remediation. Sci Total Environ. 2023;868:161376.